

# Assessing soil erosion hazard in a key badland area of Central Italy

Francesca Vergari<sup>1</sup>

Received: 15 October 2014 / Accepted: 17 September 2015 / Published online: 24 September 2015  
© Springer Science+Business Media Dordrecht 2015

**Abstract** In this work, an integrated methodology was applied to assess the water erosion hazard in Upper Orcia Valley, an area of Southern Tuscany (Italy), greatly affected by severe denudation processes, that caused the development of widespread badlands. Prediction of areas prone to *calanchi* badland development was carried out by applying a susceptibility assessment method based on conditional statistical analysis, preceded by a bivariate statistical analysis aimed at selecting the most influential causal factors of erosion. Water erosion rates at badland sites were estimated by means of an empirical statistical method, implemented to evaluate the erosion intensity (*Tu* denudation index) and based on some geomorphic parameters as independent variables. This methodology allows associating the denudation intensity to the spatial prediction. The validation procedure, based on a random partition of *calanchi* badland areas, confirmed the efficiency of the spatial zonation of the erosion hazard values. Moreover, the comparison of the estimated erosion rates with the results of decadal investigations on denudation processes affecting the study area, performed by different monitoring methods, showed the effectiveness of the estimation model. These results allowed concluding that the proposed procedure represents a useful tool to be applicable for soil protection strategy planning in land management of Mediterranean areas characterized by similar morphoclimatic features, even when direct erosion rate measures are not available.

**Keywords** Badlands · Erosion hazard · Conditional analysis · GIS · Erosion rate estimation

---

✉ Francesca Vergari  
francesca.vergari@uniroma1.it

<sup>1</sup> Dipartimento di Scienze della Terra, Università di Roma “La Sapienza”, P.le Aldo Moro n. 5, 00185 Rome, Italy

## 1 Introduction

Clayey terrains outcropping in many parts of Italy are frequently affected by accelerated erosion processes, producing landforms known as *calanchi* and *biancane*, generally considered as “badlands” (Fairbridge 1968). *Calanchi* badlands are composed of an extremely dissected, rapidly developing landscape, characterized by rill and gully landforms and a very dense dendritic drainage network (Alexander 1980). *Biancane* badlands appear as clay domes up to about 20 m high and dissected by rills (Torri et al. 1994; Torri and Bryan 1997; Calzolari and Ungaro 1998). The badlands formation and dynamics are mainly the result of the action of particularly aggressive climatic factors, such as the severe contrasts of the Mediterranean rainfall regime, on friable substrata consisting in clay, silt and sand of the Plio–Pleistocene marine cycles (Moretti and Rodolfi 2000). The morphogenetic activity is not only limited to channel erosion, but it is also due to piping and repeated superficial slides (Bryan and Yair 1982). Therefore, it should be better to consider the *calanchi* and *biancane* as the result of a “combined erosion” process (Zachar 1982). Also, areas where the natural equilibrium has been disrupted by inadequate land-use techniques can be transformed into badlands (Torri et al. 2000). The term of badlands currently refers to areas of unconsolidated sediment or poorly consolidated bedrock with little or no vegetation, which are useless for agriculture because of their intensely dissected landscape (Gallart et al. 2002).

*Biancane* generally develop on gentler slopes than *calanchi* and where lower values of amplitude of relief occur, due to the morphoevolutionary processes. Moreover, observations on present evolution *biancane* of Central Tuscany, Italy, confirm the leading role played by reticular systems of joints in dissection of the original, gently dipping surfaces (Colica and Guasparri 1990; Torri and Bryan 1997; Della Seta et al. 2009; Vergari et al. 2013a).

*Calanchi* badlands comprise very deep gullies and rills accompanied by mass movements, especially along the gully banks and gully heads. *Calanchi* are often initiated or reactivated by gully development, which may precede or follow some mass movements (Nogueras et al. 2000; Gallart et al. 2002).

The growing interest in studying badland dynamics reflects the need to increase knowledge of geomorphological processes and dynamics in badland areas (Nadal-Romero and Regüés 2010), particularly because of their importance in generating extreme water and sediment yields (Gallart et al. 2002; García-Ruiz and López-Bermudez 2009), loss and depletion of soil, landslides and, consequently, economic damages and hazardous conditions (Conoscenti et al. 2008a).

Thus, investigations aimed at monitoring and modelling gully erosion are needed as a basis for predicting the effects of environmental changes (climatic and land use) on gully erosion rates and determining the areas susceptible to gully formation, in order to properly design soil conservation plans and strategies (Gómez Gutiérrez et al. 2009a, b).

The prediction of the spatial distribution of gullies has been tackled by both assessing the topographic threshold required to be exceeded for the gully initiation (Montgomery and Dietrich 1992; Desmet et al. 1999; Kakembo et al. 2009; Nazari Samani et al. 2009; Svoray et al. 2012; Torri and Poesen 2014) and applying statistical methods to evaluate the relationships relating environmental controlling factors and the spatial distribution of gullies (Märker et al. 1999, 2011; Meyer and Martínez-Casasnovas 1999; Chaplot et al. 2005; Bou Kheir et al. 2007; Conoscenti et al. 2008a, 2013, 2014; Magliulo 2010, 2012; Akgün and Türk 2011; Conforti et al. 2011; Lucà et al. 2011). In these last investigations,

the spatial probability has never been associated with the probability of a given erosion intensity to occur in the areas predicted as prone to gullying.

One method is proposed in this paper for water erosion hazard evaluation, which is based on integration and widening of the monitoring and estimation techniques applied in the key study area of Upper Orcia Valley, Southern Tuscany, as described in previous studies (Ciccacci et al. 2003, 2008, 2009; Del Monte 2003; Del Monte et al. 2002; Della Seta et al. 2005, 2007, 2009; Vergari et al. 2011, 2013a, b; Aucelli et al. 2014). A multivariate statistical approach has been applied to evaluate water erosion hazard within the Upper Orcia Valley, where the susceptibility evaluation method based on conditional analysis (Vergari et al. 2011) was combined with the *Tu* denudation index method, an erosion intensity estimation model. By using this approach, it was possible to assess the occurrence of water erosion hazard, in terms of both the spatial and temporal probability under a given intensity in *calanchi* badlands. *Biancane* landforms, widespread in the study area, were not considered for this analysis, as they have been more frequently reshaped, even erased, by farmers than *calanchi* on the less steep slopes. So that, their natural development is more easily and frequently limited by man activities and requires more complex investigations on their genesis and transformations (Torri et al. 2013).

An empirical statistical method, the *Tu* denudation index, was chosen for the erosion estimation model in order to maintain the simplicity of the proposed analysis, also associated with the susceptibility conditional analysis. Actually, the major limits of physically based models are the large data requirements, the limited knowledge of complex processes and interactions between these processes at catchment scale (de Vente et al. 2006). Thus, they are generally more suitable for small areas or for slope-specific studies. On the contrary, empirical models are primarily based on field observations and try to characterize response from these data. The computational and data requirements for such models are usually less if compared with other types and often capable of being supported by coarse measurements. Many empirical models are based on the analysis of catchment data using stochastic techniques. In this specific study, among the empirical models, *Tu* denudation index has been selected for its tested capability of identifying the very high soil losses typical to sub-catchments greatly affected by badlands developed on uplifted Plio–Pleistocene marine clays in Italy (e.g. Ciccacci et al. 1981; Della Seta et al. 2007, 2009).

## 2 Study area

The assessment of the water erosion hazard was applied in the Upper Orcia Valley, which is the easternmost portion of the Ombrone River basin (Fig. 1a). The area is located in the Tuscan Pre-Apennines, close to Siena, North of Radicofani, and it covers about 120 km<sup>2</sup>, with the altitude ranging between 350 and 1148 m a.s.l. (Cetona Mt.). The drainage pattern and catchment shape are structurally controlled by the regional morphostructure of the Radicofani graben (Baldi et al. 1994; Carmignani et al. 1994), whose major axis is NW–SE oriented.

The geological evolution of the study area is responsible for widespread outcrops of lithological units prone to denudation (Fig. 1a). These units are Plio–Pleistocene in age and infill the NW–SE-striking graben (Baldi et al. 1994; Carmignani et al. 1994). During Quaternary, the Plio–Pleistocene marine deposits were uplifted to several hundreds of metres above the present sea level (Liotta 1996). This severe uplifting was related to pluton emplacement and widespread volcanic activity along the Tyrrhenian side (Acocella and

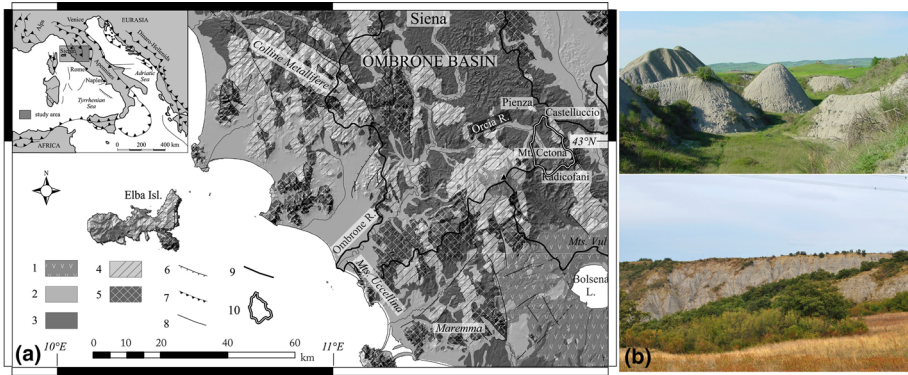


**Fig. 1** Location of the study area and geological sketch of the Tyrrhenian side of Central Italy (a) and *biancane* and *calanchi* badlands in the Upper Orcia Valley (b); (1) Quaternary volcanic rocks; (2) Quaternary undifferentiated continental deposits; (3) Plio–Pleistocene terrigenous marine deposits and Messinian evaporites; (4) sedimentary and metamorphic units of Ligurian and sub-Ligurian nappes (Trias to Lower Cretaceous); (5) sedimentary and metamorphic units of Tuscan nappe (Palaeozoic to Miocene); (6) normal fault; (7) overthrust and reverse fault; (8) undetermined fault; (9) watershed; (10) study area

Rossetti 2002), underlined by the alignment of many volcanic complexes. Quaternary uplift has been particularly strong along the southern margin of the Radicofani Graben, where locally marine deposits outcrop at 900 m a.s.l., from the Amiata-Radicofani Mt. neck, on the western side, to Cetona Mt., on the eastern slope of the study area.

The climate is temperate warm, depicted by the typical Mediterranean variability. The average annual precipitation is about 700 mm, and the mean annual temperature is around 14 °C. Annual rainfall usually varies between 500 and 1100 mm, but precipitations are concentrated during autumn and winter months, with average peak of 93 mm in November. Conversely, the summer months are hot and dry, with average monthly minimum of 31 mm in July (Della Seta et al. 2009).

The present-day geomorphic processes in the Upper Orcia catchment are firstly controlled by water erosion and secondly by gravity (Della Seta et al. 2009). The badland landforms are characterized both by “calanchi” and by “biancane” (sensu Moretti and Rodolfi 2000) (Fig. 1b). The most evident and spectacular landforms are represented by *calanchi*, which are widespread on steeper slopes, and they are typically characterized by narrow to knife-edge ridges. Moreover, residuals of a typical rounded-edged badland landscape made of *biancane* withstand the agricultural levelling practices on some gently dipping slopes. Finally, in the badland areas, micro-piping and rilling processes extensively operate on slopes, whereas landforms similar to small pediments often develop at the foot slopes (Della Seta et al. 2007).

*Calanchi* are more frequent on very steep slopes, and their growth is supported by sandy, gravel, conglomeratic or volcanic caprocks at the summit. Piping is more widespread in *biancane* sites than in *calanchi* sites in the Upper Orcia valley. Ephemeral gullies develop also on cultivated or grazing land, where they represent an important sediment source.

Human activities have strongly contributed to the landscape evolution of this region through deforestation and reforestation, grazing and farming, especially cropland abandonment, etc. These land-use changes are the most important factor triggering accelerated water erosion, tillage erosion and gravitational movements on hillslopes (Calzolari et al.

1997; Torri et al. 2002; Vergari et al. 2013b). The reshaping of badlands slopes for agricultural purposes, often through heavy machinery reaching the head of *calanchi* areas, caused preferential deep infiltration tracks which favoured the development of landslides. The rapid destruction of their typical knife-edge ridge lines is resulting due to increased gravitational processes over time, and from here shifting the evolution of the *calanchi* badland morphology from type A to type B, as classified by Rodolfi and Frascati (1979). Ciccacci et al. (2008), using field monitoring and photogrammetric techniques in the study area, confirmed that over the past 50 years *calanchi* badlands have progressively changed from type A, with sharp edges and narrow and deep gullies, to type B (with trough-floored small valleys, separated by smaller convex ridges, affected by noticeable mass movements) and, finally, to type C, characterized by higher frequency of mass movements, which almost destroy the *calanchi* ridge and fill up the small valley bottoms.

The severe denudation processes that rapidly shaped the clayey slopes of the *Crete Senesi* area have been studied over several decades by implementing field monitoring techniques or by indirect estimations of suspended sediment yield from catchments (Ciccacci et al. 1986). Both the direct and indirect quantitative geomorphic investigations were widely applied in Central Italy (Alexander 1980; Busoni et al. 1995; Ciccacci et al. 2003; Del Monte 2003; Del Monte et al. 2002; Della Seta et al. 2007, 2009; Farabollini et al. 1992; Lupia Palmieri et al. 2001; Moretti and Rodolfi 2000; Vergari et al. 2011) and led to define the *calanchi* and *biancane* badlands as erosion “hot spots” (Della Seta et al. 2007, 2009).

Geomorphological field monitoring on badlands carried out over the last 20 years showed that mean annual values of denudation rates range between 1 and 2.5 cm year<sup>-1</sup> (Del Monte 2003; Della Seta et al. 2007, 2009). Nonetheless, considerable space variability

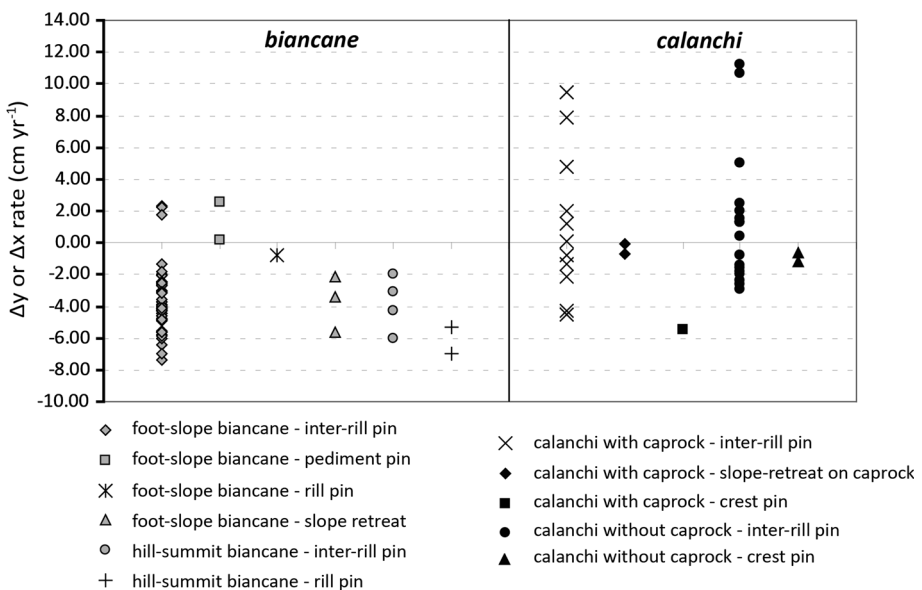


**Fig. 2** Summary of the mean erosion rates recorded at *calanchi* and *biancane* badlands sites during long-lasting geomorphological studies in Tyrrhenian side of Central Italy (updated from Della Seta et al. 2009). Both vertical ( $\Delta y$ ) and horizontal ( $\Delta x$ ) variations of ground level were recorded at different sites and positions on slopes

of ground-level changes was observed along hillslope (Fig. 2): between  $-1$  and  $-8$   $\text{cm year}^{-1}$  at different positions on *biancane* slopes, between  $+11$  (net accumulation) and  $-5$   $\text{cm year}^{-1}$  at different positions on *calanchi* slopes (Aucelli et al. 2014). The dominant role of different processes involved in shaping these different badlands types causes differences of in-site erosion/accumulation budget. As to the off-site effects, the estimated values of mean annual suspended sediment load for the major catchments increase exponentially with the ratio of badlands area to the whole catchments (Della Seta et al. 2009). Instant suspended load measurements at the outlet of some major catchments have testified for the pulsating connectivity of the small badlands catchment to the major streams. In particular, few extreme denudation events can deliver enough sediment in the major streams to reach the overall estimated mean annual suspended sediment load (Della Seta et al. 2007, 2009).

### 3 Materials and methods

The statistical susceptibility evaluation method, described by Vergari et al. (2011) for the landslide susceptibility assessment, has been applied to the denudation landforms due to run-off, *calanchi* badland areas, in order to evaluate the water erosion spatial proneness of the study area. The relation between the *calanchi* badland areas and the distribution of the values of some potential quantitative environmental parameters was explored to achieve this goal. As illustrated in Fig. 3, the water erosion hazard assessment was obtained by combining the evaluated spatial prediction with the estimation of the water erosion rates of the unstable landforms, performed by using the “*Tu* denudation index” (Ciccacci et al. 1981, 1986; Della Seta et al. 2009; Vergari et al. 2014). Vector data sets in GIS environment were used to obtain vector susceptibility outputs, which are expected to be less fragmented than the raster ones and, consequently, easier to be interpreted by users. For temporal uniformity, all the input data (Digital Elevation Model, drainage network and *calanchi* inventory map) were derived from the topographic maps at scale 1:10,000 (1994 Regional Topographic maps) or other contemporaneous data.

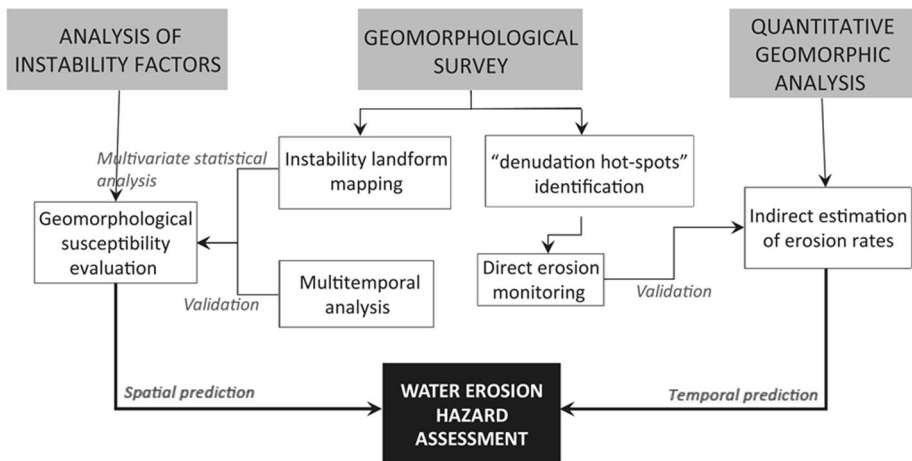


**Fig. 3** Conceptual frame of the proposed method for water erosion hazard evaluation

### 3.1 Input data thematic maps

Aerial photograph interpretation and field survey have allowed the assessment of the spatial distribution of water erosion processes, resulting in an inventory map of *calanchi* badland landforms (Fig. 4). The mapped *calanchi* badland area consists of slope units widely affected by gully erosion, which represent micro-basins.

*Calanchi* landforms are the most evident and spectacular ones related to gully erosion in the study area, almost exclusively developed into clayey layers, with a channel network mainly by dendritic pattern. The *calanchi* are often characterized by landslide escarpments at their headwater, which promote concentration of surface running water (Morgan 2005; Conforti et al. 2011). The geomorphological survey inside the badland areas from the Upper Orcia valley shows that small mass movements generate smoothed ridges within the main gullies. Moreover, along badland slopes micro-piping and rilling processes operate, whereas mud flow cones are often accumulated at the mouth of various order drainage channels.

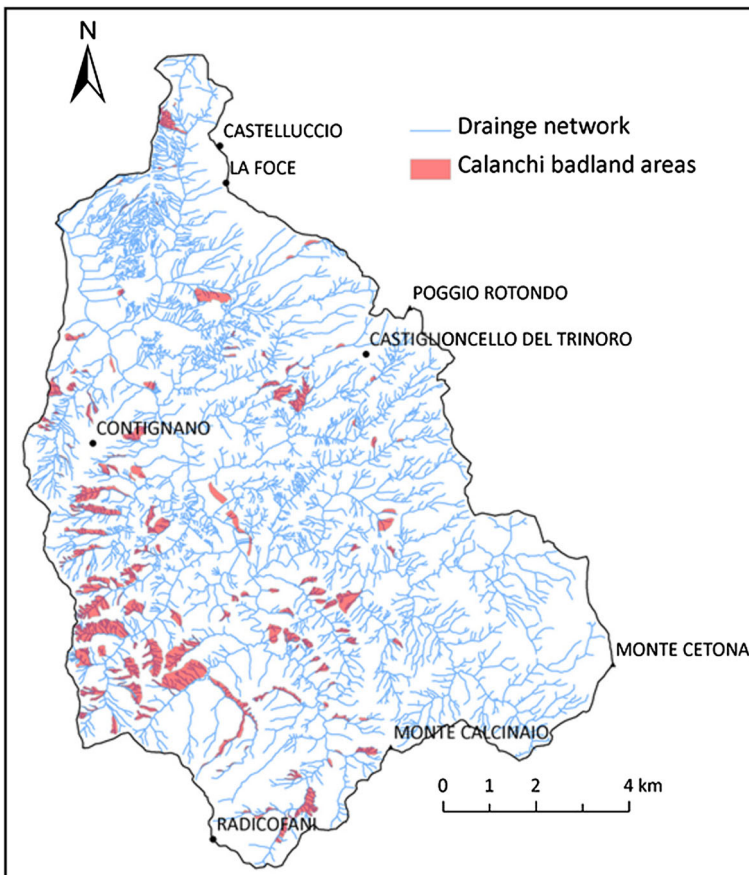


**Fig. 4** Distribution of *calanchi* badlands areas overlaid to the drainage network map of Upper Orcia Valley

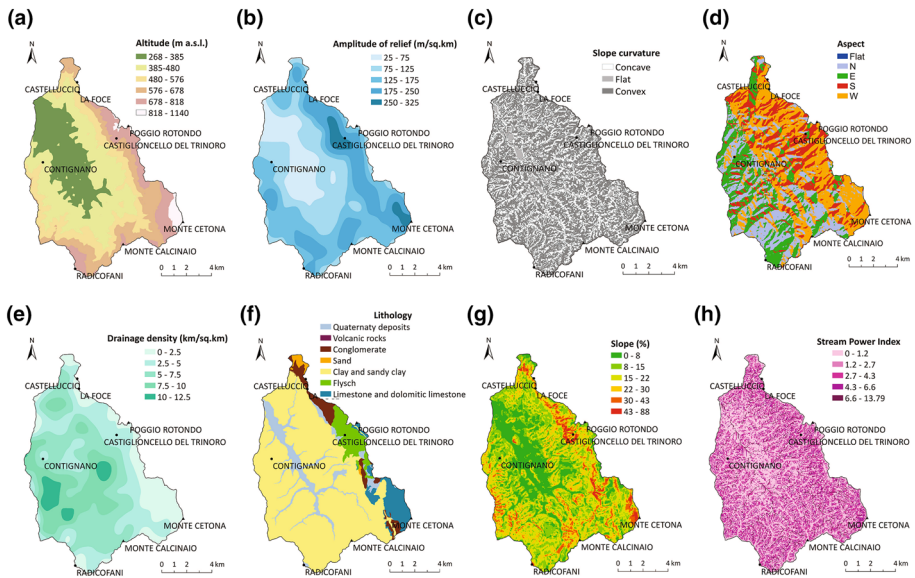


**Fig. 5** Potential causal factors considered in the water erosion hazard evaluation in the Upper Orcia Valley: **a** altimetry, **b** amplitude of relief, **c** slope curvature, **d** aspect, **e** drainage density, **f** lithology, **g** slope, **h** stream power index

Figure 5 shows that eight parameters have been considered to quantify the potential erosion causal factors, namely altitude (A), amplitude of relief (AR), slope curvature (C), aspect (A), drainage density (D), lithology (L), slope gradient (S) and stream power index (SPI). A DEM with 25-m resolution was used to derive the topographic factors. The output raster layers were then aggregated in 50-m cell-sized grids to avoid the excessive fragmentation of map units and to reconstruct the average slope conditions, as the terrain conditions preceding the instability events should be considered for a well-structured susceptibility analysis.

Altimetry was taken into account to investigate the possible concentration of badland areas in particular elevation intervals (Fig. 5a). The highest altitude values are concentrated along the south-eastern divide corresponding to the horst bordering the Radicofani graben, to the east and to the strongest Quaternary uplift of the Plio–Pleistocene marine deposits, to the South.

The amplitude of relief map illustrates the maximum difference in height per unit area ( $1 \text{ km}^2$ ) and was derived by raster calculations from the DEM in ArcGIS environment (Fig. 5b). The results are visualized using contour lines and deriving from them a polygonal vector data set, which was classified by using the natural breaks method. This parameter provides a measure of fluvial erosive action. Other conditions being equal, it was verified that the spatial distribution of this parameter can provide information about vertical displacements such as local fault activity or regional uplift (Della Seta et al. 2004). In addition, the highest AR values are clustered along the basin's eastern divide, where the western flank of the Castelluccio–Cetona Mt. horst is bounded by fault scarps.



Slope curvature was investigated with respect to its effect on badland triggering and development (Fig. 5c). The term curvature is theoretically defined as the rate of change of slope gradient or aspect, usually in a particular direction (Wilson and Gallant 2000). The curvature of the surface is computed on a cell-by-cell basis, as fitted through that cell and its eight surrounding neighbours. Curvature is the second derivative of the surface or the slope of the slope. Positive values of curvatures define convexity, and the negative values of curvatures characterize concavity of slope curvature. Values of curvatures around zero indicate flat surfaces.

The aspect map was derived using the terrain analysis tool in GIS environment (Fig. 5d). The 50-m cell-size raster output was classified into five groups of A (flat, N, S, E, W). The horizontal areas do not have significant extent, while the other classes are all well distributed in the study area.

The drainage density map was derived by calculating the cumulative length of stream segments of the drainage network digitized from 1:10,000 topographic maps (CTR of Tuscany Region) falling within unit areas of 1 km<sup>2</sup> (Fig. 5e). As for the amplitude of relief map, contour lines were derived and a polygonal vector data set was classified into equal intervals of  $D$  (2.5 km km<sup>-2</sup>).  $D$  is a parameter that indirectly accounts for the erodibility and permeability of outcropping rocks, the degree of tectonization, the vegetation cover, the slope gradient, and the mean annual rainfall in the drainage basin. Due to the widespread outcrop of clays amounting 73 % of the total area, more than half of the study area is characterized by high or very high  $D$  values, between 5 and 12.5 km km<sup>-2</sup>. Moreover, the heads of several catchments are affected by badlands, where run-off is absolutely dominant with respect to infiltration.

The lithological map was drawn by grouping the outcropping rocks according to their response to denudation processes (Fig. 5f). The geological setting of the area is well known, and the rock units reported in the existing geological map have been grouped into eight lithological units.

The slope map was derived from the 25-m cell-sized DTM by using the analysis tools in ArcGIS 3D Analyst (Fig. 5g).  $S$  values were grouped into six classes using the Jenks' natural breaks method (Jenks 1967), and the raster data set was converted to a vector format. The first four classes are widespread within the study area (16–26 %), whereas classes 5 and 6 comprise mainly the most coherent lithologies crop.

The stream power index (SPI), as shown in Fig. 5h, is a measure of the erosive power of streamflow based on the assumption that discharge is proportional to the specific catchment area ( $A_s$ ) (Moore et al. 1991). The map was carried out by applying the following formula to each cell, using Raster Calculator in ArcGIS:

$$\text{SPI} = \ln[A_s \times \tan(S)]$$

where  $A_s$  is the specific catchment area in square metres and  $S$  is the slope gradient in radians. When  $S$  was  $>30$  %,  $\tan(S)$  was substituted by  $\sin(S)$ , as suggested by Torri and Poesen (2014). Stream power index can be used to describe the potential run-off erosion at a given point of the topographic surface. That means as the catchment area and slope gradient increase the amount of water delivered by upslope areas and the velocity of run-off increase, hence stream power index and erosion risk are higher. Thus, the SPI is one of the main factors controlling slope erosion processes, since erosive power of overland flow directly influences slope undermining and river incision by streamflow. It is also indicative of the potential energy available to entrain sediment, and therefore, the areas with high stream power indices have great potential for erosion

(Bagnold 1966; Yang and Stall 1974; Moore et al. 1991; Nefeslioglu et al. 2008; Kakembo et al. 2009; Florinsky 2012).

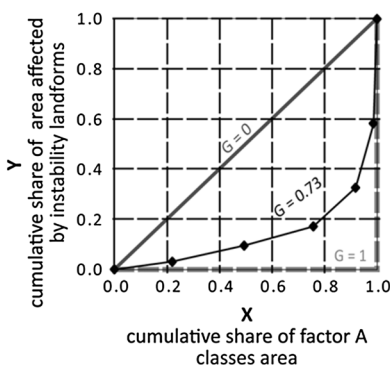
### 3.2 Water erosion susceptibility assessment method

The susceptibility evaluation method, proposed by Vergari et al. (2011) for landslide susceptibility assessment, was here applied to quantify the probability of the study area to host water erosion landforms. This procedure is based on the statistical conditional analysis (Bonham-Carter et al. 1989; Carrara et al. 1995), used to quantify the multi-variate relationships between environmental attributes (or instability causal factors) and past and present instability landforms occurrence. The analysis is preceded by an unbiased bivariate statistical procedure for selecting the most influential causal factors (Vergari et al. 2011).

In particular, the factor selection (Fig. 6) consists of measures of inequality distributions (Gini 1914) and computation of Lorenz curves (Lorenz 1905). The Lorenz curves are constructed after the intersection of each causal factor map with each instability landform map, in this case the *calanchi* landforms. Gini's index of inequality and Lorenz curves is applied to understand the distribution of occurred hazardous events within the different classes of influencing factors: each point on the Lorenz curve represents the cumulative area affected by a given hazardous event type versus the cumulative portion of the study area characterized by a certain class of a given potential causal factor. The line of perfect inequality (dotted line in Fig. 6a) represents the situation in which all the landforms are clustered in a single factor class, whereas their homogeneous distribution in all the factor classes is represented by the line of perfect equality (the 1:1 solid line in Fig. 6a).

The Gini coefficient ( $G$ ) is graphically represented by the area between the line of perfect equality and the computed Lorenz curve, and it is expressed as the portion of the area between the line of perfect equality and the line of perfect inequality (Gini 1914). This area can be approximated with trapezoids and can be calculated using the following formula:

(a) Lorenz curve for the causal factor A:



(b) FACTOR SELECTION with Gini coefficient ( $G$ )

$G$  quantifies the difference between the observed Lorenz curve and the line of perfect uniformity distribution ( $G=0$ ):

$$G = 1 - \sum_{n=1} (X_n - X_{n-1})(Y_n + Y_{n-1})$$

For each instability landform the mean from  $G$  values obtained for all the potential causal factors is calculated and the factors with  $G$  above the mean are selected.

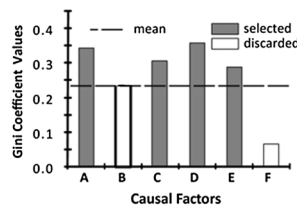


Fig. 6 Factor selection procedure (modified after Vergari et al. 2011)

$$G = 1 - \sum_{n=1}^N (X_n - X_{n-1})(Y_n + Y_{n-1}) \tag{1}$$

where  $n$  = factor class,  $N$  = total number of factor classes,  $X_n$  = cumulative portion of the study area characterized by the factor class  $k$ , with  $X_0 = 0$ ,  $X_N = 1$ ,  $Y_n$  = cumulative portion of instability landform area falling in the factor class  $k$ , with  $Y_0 = 0$ ,  $Y_N = 1$ .

For each instability landform type analysis, a factor is selected if the corresponding  $G$  value is higher than the average of the coefficient values of all of the considered factors (Fig. 6b). In this way, independently of the absolute  $G$  values, factors with  $G$  higher than the mean value will be more discriminant than the others for the same instability process type occurrence in the study area.

The susceptibility evaluation for each instability landform type has to be preceded by a careful evaluation of the best factor classification method.

Once the causal factors are finally selected for each instability type, the conditional analysis allows obtaining a number of vUCUs map units (vector Unique Condition Units) from all of the possible selected factor combinations in the study area. Conceptually, these map units correspond to the Unique Condition Units (UCUs) proposed by Carrara et al. (1995). The susceptibility index for each vUCU, used to draw up the susceptibility map, is successively calculated using the Bayesian interpretation of probability. The importance of applying conditional probability models has been strongly emphasized in the Earth Sciences literature, especially for predicting hazardous events or mapping mineral potential (Bonham-Carter et al. 1989). Afterwards, these models have been applied by several authors for landslide susceptibility evaluation (Chung and Fabbri 1999; Irigaray Fernández et al. 1999; Clerici et al. 2006, 2010; Zêzere et al. 2004; Conoscenti et al. 2008b) and gully erosion susceptibility (Conoscenti et al. 2008a; Conforti et al. 2011). The Bayes rule allows the probability of future hazardous events to be predicted once the area of each vUCU affected by past events is known. The Bayes rule specifies a prior probability, which is then updated in the light of new relevant data (called “likelihood” in Bayesian theory). In the study case, this means that the simple attribution of an a priori determined probability has to be updated considering information on past events. Thus, the susceptibility index corresponds to the conditional or posterior probability  $P(f|vUCU)$ , which is the probability of the occurrence of a hazardous event type, given a certain combination of selected causal factors (vUCU).

The susceptibility index ( $S_{index}$ ) for each  $i$ th vUCU can be computed more easily because it corresponds to the ratio of the instability landform area affecting vUCU $_i$  ( $A_{f,vUCU_i}$ ) to the area of vUCU $_i$  ( $A_{vUCU_i}$ ):

$$S_{index} = \frac{A_{f,vUCU_i}}{A_{vUCU_i}} \tag{2}$$

The  $S_{index}$  values for each vUCU indicate the probability of the instability process type occurrence conditioned by the concomitant presence of the selected causal factor categories.  $S_{index}$  of a vUCU may be expressed by a percentage and thus theoretically ranges between 0 and 100 %, where 100 % is the maximum probability of a hazardous event, given by the complete coverage of the vUCU by hazardous events.

### 3.3 Water erosion intensity estimation

In order to estimate the erosion intensity at the scale of slopes where badlands develop, an adjustment of a methodology implemented to predict catchment scale erosion rates is here proposed. Ciccacci et al. (1981, 1986) obtained empirical equations for the “*Tu* denudation index” by statistically correlating the values of measured suspended sediment yield at the outlets of several Italian catchments to some geomorphic and climatic parameters, such as drainage density, pluviometric regime indices, mean annual discharge and other parameters expressing the hierarchical structure of the drainage network (Fig. 7). The suspended sediment yield (*Tu*, t km<sup>-2</sup>year<sup>-1</sup>) seems to be the most suitable expression of erosion rate, because it is easily measured and represents approximately 50 % under arid and semi-arid climates to 90 % under humid climates of total sediment yield by rivers (Cooke and Doornkamp 1974; Lupia Palmieri 1983). The “denudation index” (*Tu*) showed noticeable spatial variability of estimated denudation, with the highest *Tu* values indicating erosion “hot spots”, represented by small sub-catchments affected by badlands developed on uplifted Plio–Pleistocene marine clays in Italy (Della Seta et al. 2009).

Given these encouraging results, during the last years some attempts have been made to perform more detailed zonations of the predicted denudation rates, called “*Tu* grid analysis” (Aucelli et al. 2010; Maerker et al. 2012; Vergari et al. 2014), in order to better zoning the negative ground-level changes on badland sites within the catchment area (cm year<sup>-1</sup>). To this end, Eqs. (3) and (4) derived by Ciccacci et al. (1981) were used, where only the density (*D*) of 14 Italian sampled drainage basins has been considered as the independent variable:

$$\log Tu = 0.35312D + 1.43225 \quad R^2 = 0.962 \quad (\text{with } D < 6 \text{ km km}^{-2}) \quad (3)$$

$$\log Tu = 2.93936 \log D + 1.13430 \quad R^2 = 0.950 \quad (\text{with } D > 6 \text{ km km}^{-2}) \quad (4)$$

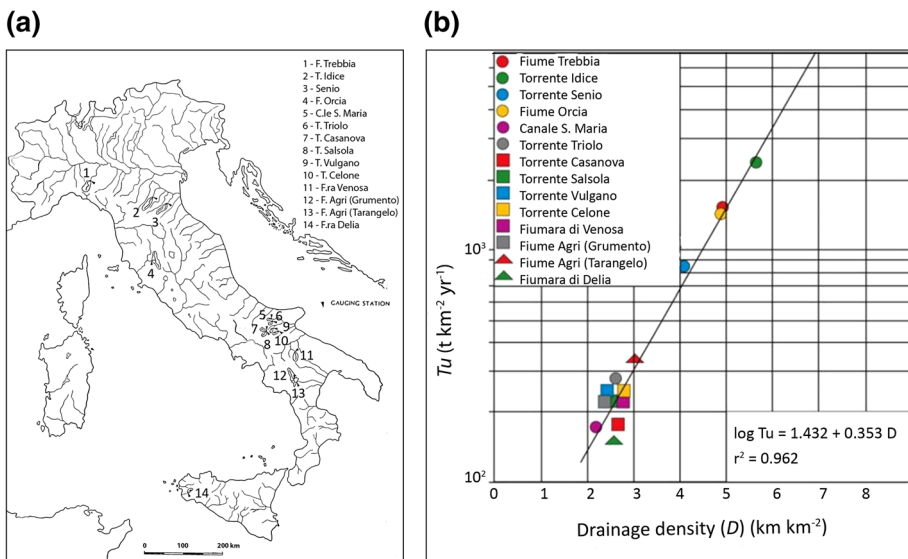


**Fig. 7** Italian sampled drainage basins used to carry out the “*Tu* denudation index” (a) and the empirical equation proposed by Ciccacci et al. (1981) (b)

$D$  parameter synthetically expresses many of the factors controlling erosion entity, namely (a) it is strongly depending on climatic conditions and terrain topography; (b) it is tied to the type and density of vegetation cover; (c) it can be partially modified in response to human activity; (d) it is a function of rock permeability and fracturing degree, synthesizing the erodibility level of the sedimentary substratum outcropping in the studied areas.

Ciccacci et al. (1981, 1986) showed how these equations succeeded in estimating the suspended sediment yield of Upper Orcia Valley measured at the Monte Amiata Hydrological Station with a 6 % error.

The Upper Orcia catchment was divided into a grid of 1 km<sup>2</sup> cells to evaluate the  $Tu$  index for unit areas. Then, the grid was spatially shifted diagonally by  $\sqrt{2}$  km to double the number of cells for  $Tu$  computation and thus the analytical detail, one value for each unit area of 0.25 km<sup>2</sup>. The  $D$  value for each cell was calculated from drainage network digitized from topographic maps at scale 1:10,000. The  $Tu$  index value (t km<sup>-2</sup> year<sup>-1</sup>) was estimated for each cell, corresponding to the estimated sediment output from the same cell. The  $Tu$  value was then converted into the average negative ground-level change of the cell (cm year<sup>-1</sup>), assuming a mean bulk density of outcropping clays equal to 1.6 t m<sup>-3</sup>. This average value was chosen, considering that bulk density in arable land from the study area is about 1.4 t m<sup>-3</sup> (De Alba et al. 2006), while in regolith crust of the badland areas it has been quantified at 1.8 t m<sup>-3</sup> (Torri and Bryan 1997). The so-estimated erosion rates were assigned to the cells' centroids to get a point cloud to be used for geostatistical interpolations, thus obtaining the estimated erosion rate map of the Upper Orcia catchment. The spline interpolation method was applied, since the interpolated surface can exceed the known value range, but must pass through all of the sample points. The smoothing effect of the interpolator was in this case applied, since the input data do not represent point values measured in the field but values over unit areas.

### 3.4 Validation procedure

While field erosion monitoring data collected in some of the badlands were used to validate the estimation of the erosion rates, a validation procedure based on a spatial random partition strategy was applied to test the effectiveness of the susceptibility predictive model. The method proposed by Chung and Fabbri (2003) for landslide susceptibility model validation was applied, aimed at constructing both the prediction-rate and the success-rate curves. This method requires partition of the instability landform database into a *training subset* and a *test subset*, considering the second one as the unknown future target pattern of instability events and, thus, pretending that the instability events of the test subset have not yet developed. When possible, a temporal partition of the landforms is recommended by using the air photograph mosaic of a specific year within the inventory time span. When not possible, an alternative is the one here adopted that is based on random spatial partition of the instability landforms. Once the partition of the landforms affected by water erosion is carried out, the susceptibility analysis already applied to the whole landform inventory can be shifted to the only training subset, thus obtaining the training susceptibility map. Finally, the distribution of the test subset landforms is compared with the training susceptibility map in order to construct the prediction-rate curve. Success-rate and prediction-rate curves plot the percentage of the study area in each susceptibility class against the percentage of instability landform area in the same class.

While the success-rate curve is constructed considering the same inventory used to construct the susceptibility model and hence represents a measure of model fit, the prediction-rate curve is built considering independent instability landform information (i.e. by intersecting the training susceptibility map and the instability landforms of the test subset) and measures the prediction skill of the classification.

Since this study used vector layers, the curves were constructed by plotting the cumulative area of vUCUs, ordered by decreasing  $S_{index}$  values (x-axis) and versus the cumulative area affected by instability processes within each vUCU (y-axis).

Ideally, the tangent of a *prediction-rate curve* should be monotonically decreasing to indicate that the most hazardous classes predict most of the “future” events, and the trend regularly decreases with the gradual reduction of the susceptibility value. However, as described by Chung and Fabbri (2003), empirical *prediction-rate curves* usually do not satisfy this condition. A 1:1 trend of the prediction-rate curve indicates that the prediction map is randomly generated. Thus, the further the prediction-rate curve is far from a straight line, the more the susceptibility estimation is significant. Moreover, the steeper the curve is

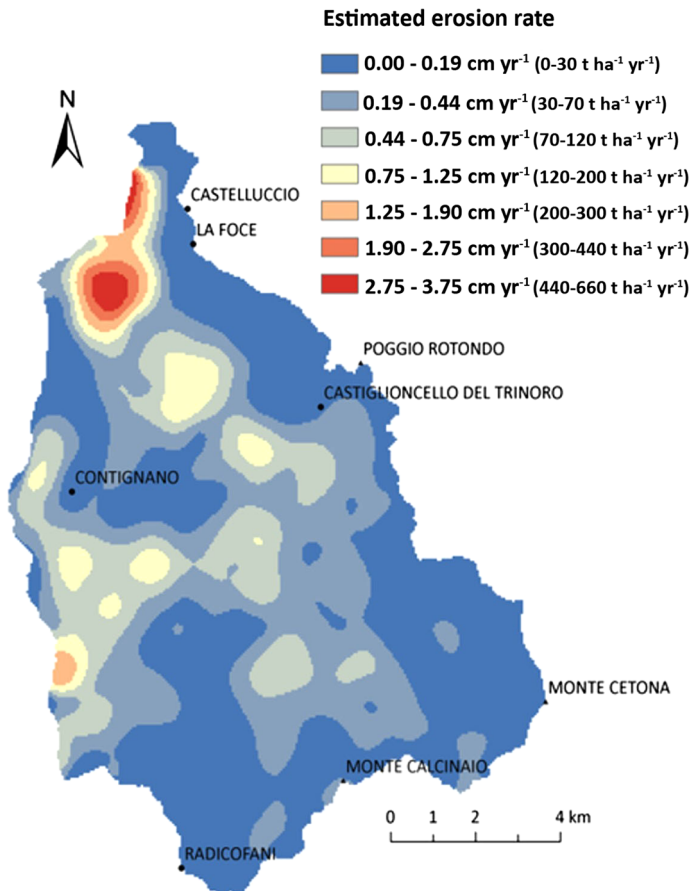


**Fig. 8** Estimated erosion rate map of Upper Orcia Valley, performed by applying the *Tu* grid analysis

in its first part, the greater the predictive power of the prediction map (Remondo et al. 2003).

## 4 Results

### 4.1 Erosion rates estimation in the *calanchi* badlands

Starting from the drainage network of the Upper Orcia Valley, digitized from 1:10,000 topographic maps (CTR, Tuscany Region), the erosion rates map was carried out through the *Tu* grid analysis and using Eqs. 3 and 4 (Fig. 8). The map shows that the highest erosion rates correspond to the *biancane* and *calanchi* badlands or to some areas where badlands have been remodelled for agricultural purposes.

The map was then validated by comparing the estimated erosion rates with those measured during the last 20 years. The graph from Fig. 2 summarizes the average ground-level changes measured in the last two decades using erosion pins and photogrammetric analysis located in different erosion landforms. The average measured erosion rate, only due to run-off, in badlands areas was 1.5–2.5 cm year<sup>-1</sup> that corresponds to the range 240–400 t ha<sup>-1</sup> year<sup>-1</sup>, values comparable to the estimated ones.

Taking into account the only drainage network of the areas affected by *calanchi* badlands, whose mean density value is 16.62 km km<sup>-2</sup>, a zonal statistics analysis allowed to calculate an average erosion rate exceeding 2 cm year<sup>-1</sup> (320 t ha<sup>-1</sup> year<sup>-1</sup>) in these areas. This value agrees with the magnitude order of erosion rates measured at *calanchi* badlands sites of Central Italy (Della Seta et al. 2009; Vergari et al. 2013a, b; Aucelli et al. 2014).

### 4.2 Factor selection

The most influential causal factors in determining water erosion effects have been selected by applying the factor selection procedure described in Sect. 3.2. Figure 9a shows the Lorenz curves for the considered eight potential causal factors, computed after the intersection of the badland inventory map with each of the factor maps.

Altimetry, drainage density, amplitude of relief and slope are the selected factors (Fig. 9b).

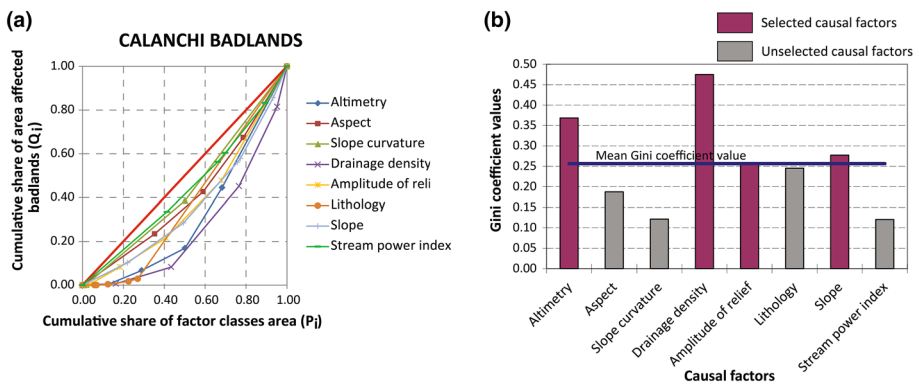


**Fig. 9** Lorenz curves for the considered potential causal factors with the Gini coefficient values for each factor (a) and histogram showing the Gini coefficient values and the selected causal factors (b)

Drainage density is the most important causal factor in discriminating areas affected by badland erosion, as high  $D$  values identify areas where overland flow is favoured and run-off increases. Altimetry is the second most important factor, since most of *calanchi* areas are stretching up to 700 m a.s.l., which is the maximum elevation of clayey outcrops in the study area. At higher altitudes, other more resistant layers outcrop. This means that even if lithology was discarded, the information provided by the lithology map is still beheld in the model. As for slope and amplitude of relief, *calanchi* badlands are concentrated in medium slope gradient values (15–40 %) and in 100–200 m  $\text{km}^{-2}$  amplitude of relief interval. Higher amplitude of relief values characterizes the eastern part of the study area, where calcareous outcrops prevail.

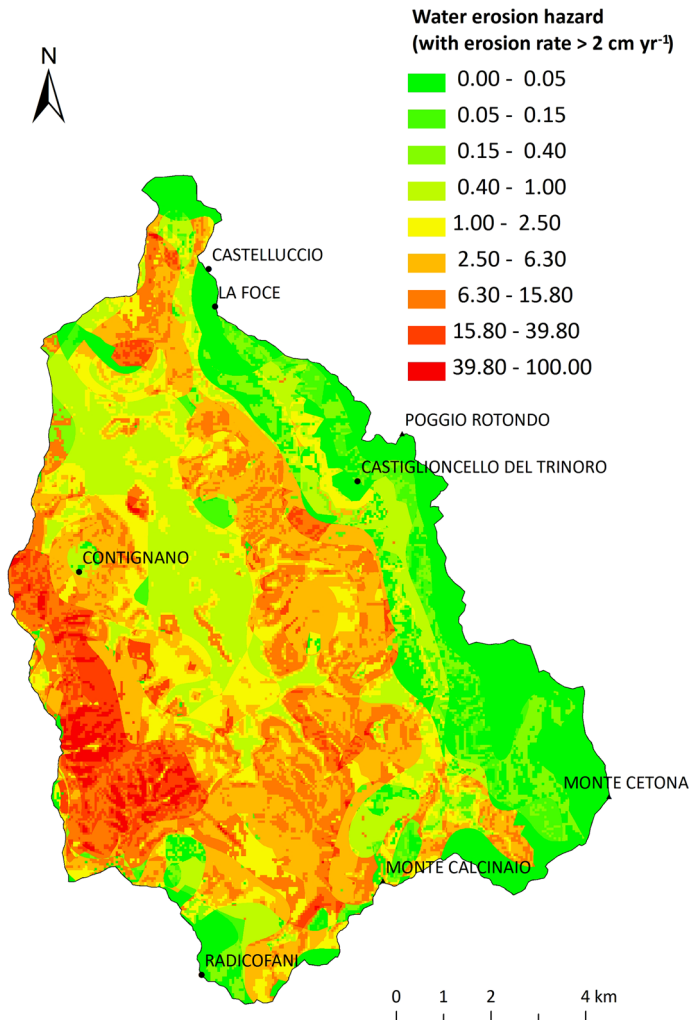


**Fig. 10** Water erosion hazard map of Upper Orcia Valley. The probability of the study area of being affected by erosion rates higher than  $2 \text{ cm year}^{-1}$  ( $320 \text{ t ha year}^{-1}$ ) is zoned



### 4.3 Water erosion hazard assessment

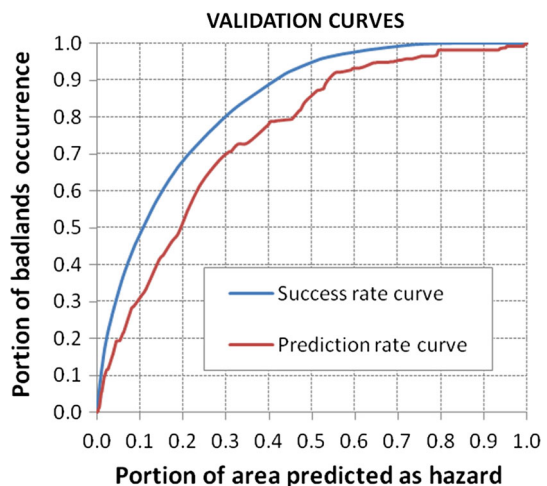
By intersecting the selected causal factors, the water erosion hazard map was carried out (Fig. 10). The hazard values represent the conditional probability of the occurrence of *calanchi* badland erosion with a soil erosion rate higher than  $2 \text{ cm year}^{-1}$  ( $320 \text{ t ha}^{-1} \text{ year}^{-1}$ ). Hazard values were classified into nine classes of increasing hazard level. The highest hazard values are located in the western sector of the study area, where clayey outcrops are characterized by very high slope gradient. At present, most of that area is totally affected by badlands and, therefore, included in the very high hazard class. However, in this sector a wider land is very prone to water erosion, and the development of badlands is frequently restrained by the agricultural land remodelling practices.

### 4.4 Validation results

In order to validate the susceptibility map by drawing the prediction-rate and the success-rate curves, the gully areas data set has been split into two subsets using a random partition (Chung and Fabbri 2003). One subset (training set, 70 % of all water erosion landforms) has been used to obtain the training susceptibility map, and the second subset (test subset with the remaining 30 %) has been used to validate the susceptibility map. The selected environmental factors used to obtain the training susceptibility map were altimetry, drainage density, lithology and slope.

Both the success-rate and the prediction-rate curves for the Upper Orcia Valley show a high gradient in the first part and smoothly decrease monotonically (Fig. 11). The prediction curve shows that 70 % of the total badland area of the test subset falls within 30 % of the areas predicted as the most prone to badland development. This result confirms both the validity of the susceptibility method and the high spatial correlation between controlling factors used for the analysis and the instability landform distribution. Furthermore, the validation procedure results show that the predictive power of the model is generally satisfactory. Therefore, about 85 % of the instability landform area of the training subset is correctly classified falling in high and very high susceptibility classes.

**Fig. 11** Validation curves



The estimated erosion rates, already compared with those measured during field monitoring with pins over the last 20 years in the badland areas, were further validated through their comparison with the volumetric estimation of material removed by denudation processes, carried out in a small sub-catchment of the study area in a previous study (Aucelli et al. 2014). The Landola sub-catchment, widely affected by water erosion landforms, corresponds to the area between the Radicofani and Contignano towns, where the highest susceptibility index values have been predicted. During the Landola investigations, multitemporal photogrammetric analysis was performed in order to evaluate the time and space evolution of erosion processes mainly triggered by surface run-off and landslides for about the last 60 years. The analysis allowed to calculate an average erosion rate of  $1.2 \text{ cm year}^{-1}$  (about  $200 \text{ t ha}^{-1} \text{ year}^{-1}$ ) in the whole sub-catchment, but higher average values were obtained when considering only the areas affected by badlands (up to  $6 \text{ cm year}^{-1}$ ). Centimetric erosion rates were also observed by De Alba et al. (2006) on croplands, where tillage erosion is caused by uphill and downhill farming, especially mouldboard ploughing.

## 5 Discussion

The most important innovative aspect of this investigation refers to the proposal of the integration of soil erosion susceptibility analysis with water erosion rate estimation method. Thus, the water erosion hazard assessment is obtained that can predict the probability of the area to develop water erosion landforms characterized by a given erosion rate. The choice of the Upper Orcia Valley as test area was driven by the wide availability of multitemporal morphodynamics studies and erosion monitoring data covering decadal periods. This allowed validating estimates of the denudation intensity and, given the encouraging results, to propose the methodology for similar Mediterranean badlands where long monitoring series are not available.

It has to be underlined that the proposed estimation of erosion rates has been validated for water erosion contribution to soil losses, monitored by means of erosion pins in the studied badland areas (Ciccacci et al. 2003, 2008; Della Seta et al. 2007, 2009; Vergari et al. 2013a). Even so, higher denudation in the *calanchi* sites can be locally due to considerable removal of material caused by mass movements, as resulted after multitemporal digital photogrammetric analysis (Aucelli et al. 2012, 2014). Moreover, further investigations could extend the applicability of the erosion rate estimation model to other land uses than bare soils under badlands (e.g. cropland).

The obtained erosion rates confirm how these Mediterranean badlands can be considered “erosion hot spots”, as they were defined by Della Seta et al. (2007, 2009). If compared to the soil erosion rates estimated at European and Mediterranean scales by using different techniques (Grimm et al. 2003; Cerdan et al. 2010; Maetens et al. 2012), the entire study area shows considerable higher values, resulting from the very high dispersivity of the clays (Vergari et al. 2013a). In particular, for the whole Italian territory, Cerdan et al. (2010) estimate a mean erosion rate of  $2.3 \text{ t ha}^{-1} \text{ year}^{-1}$ , contributing to the 12.5 % of the total European erosion, even if when considering the different land-use categories bare land clearly shows the highest values of  $15 \text{ t ha}^{-1} \text{ year}^{-1}$  on average. These authors underline that the Italian Apennine slopes show the highest estimated erosion rates exceeding  $20 \text{ t ha}^{-1} \text{ year}^{-1}$  in the Mediterranean zone, a trend confirmed by Van Rompaey et al. (2005). Considering the study area, it is included in the European and Italian zones

with the highest potential soil erosion risk identified by Grimm et al. (2003), showing an annual approximate soil losses exceeding  $20\text{--}40\text{ t ha}^{-1}\text{ year}^{-1}$ . All these studies were carried out at very different spatial scales from that of this study, as they investigate very large areas and at very low spatial resolution. Moreover, their environmental contexts are very wide, as Europe and the Mediterranean include a great variability of climates, land uses, topography, outcropping lithologies and soils.

As recently underlined by García-Ruíz et al. (2015), there is a negative relationship between the erosion rate and the size of the study area involved. Thus, the results of this study can be more properly compared to areas with similar environmental conditions, such as the Mediterranean badlands. Taking into account these particular landscapes, the high denudation intensity measured and estimated in Upper Orcia Valley is not so surprising. In fact, a review of monitoring investigations, performed in different Mediterranean badland sites (France, Spain, Southern Italy) and with different techniques (erosion pins, profile metres, sediment traps, volumetric analyses, instrumented catchments), shows erosion rates ranging between  $100$  and  $600\text{ t ha}^{-1}\text{ year}^{-1}$ , depending on the site altitude and average annual precipitation amount and seasonality, and reaching more than  $1000\text{ t ha}^{-1}\text{ year}^{-1}$  when very small badlands areas are considered (Bufalo and Nahon 1992; Brochot 1993; Martínez-Casasnovas and Poch 1998; Regüés et al. 2000a; Gallart et al. 2002; Martínez-Carreras et al. 2007; Sirvent et al. 1997; Nadal-Romero et al. 2008; Nadal-Romero and Regüés 2010; Piccarreta et al. 2012). In Mediterranean badland areas, Nadal-Romero et al. (2011, 2014) noticed that for less than 10 ha areas erosion rates are very high because of the absence of sediment storage in badlands. Instead, in the catchment larger than 10 ha the erosion rate decreases nonlinearly as the area increases because sediment is trapped in the valley bottoms and in the footslopes.

As for the erosion susceptibility analysis, the validation confirmed the efficiency of the factor selection procedure, which allowed using few causal factors without losing information on the indirect influence of the discarded ones. For example, the lithology factor was discarded, but its information is still indirectly provided by the selected causal factors, which are spatially correlated with it. Actually, clayey outcropping deposits, being barely permeable, are characterized by high values of drainage density and are concentrated in the altimetry classes up to 700 m a.s.l. More resistant layers outcropping at higher altitude favour low drainage density, high amplitude of relief and steeper slopes. Thus, the use of the lithology factor in the analysis would have resulted in the inclusion of redundant information about the badland distribution. At the same time, the aspect factor that might be used by an expert operator for its well-known influence on badland distribution was not selected. Slope aspect clearly plays a relevant role in controlling regolith moisture and its influence on weathering and erosion processes (Yair and Lavee 1985) with a greater strength from arid to semi-arid badlands, as sunny aspects show poor or null vegetation cover causing badlands typical asymmetry (Kirkby et al. 1990; Solé et al. 1997; Cantón 1999). As the annual precipitation increases, exceeding 700 mm in humid Mediterranean badlands, there is enough water to allow development of vegetation cover, which limits high erosion rates more than dryness linked to aspect (Richard and Mathys 1999; Regüés et al. 2000b; Gallart et al. 2002; Nadal-Romero et al. 2014). The factor selection procedure used in this study revealed that, differently from other badland areas, badlands are not so much concentrated on south-facing slopes. The geomorphological survey in the area showed that hillslope aspect is much more important in determining the different denudation processes acting at badland sites, resulting in the two types of *calanchi* morphology described by Rodolfi and Frascati (1979) and Moretti and Rodolfi (2000), namely the south-facing *calanchi* are more affected by rill and gully erosion, producing the type A

morphology (with steep, deeply incised, sharp knife-edged ridges, and a very dense drainage pattern), while in the north-facing *calanchi* frequent shallow landslides coexist with water erosion, resulting in the type B morphology, characterized by gentler slopes and smooth divides with a less dense drainage system.

The obtained results confirm that the unbiased selection of controlling factors is a crucial phase for geomorphological susceptibility evaluations (Vergari et al. 2011). However, both the heuristic and the statistical choice of causal factors require previous knowledge of the main causes of geomorphological instability. That means the potential factors must be not only spatially correlated with the distribution of the target landforms but also in cause/effect relations with them. This can sometimes lead to the exclusion of variables spatially well correlated with hazardous events distribution but representing an instability process effect more than its cause. This was the reason for which the land-use map was not included in the list of the potential causal factor in this study. Farming in the Upper Orcia Valley represents the most common anthropic activity, but its distribution is strongly driven by the extension of soil erosion processes. A lot of cropland is subjected to soil erosion or results from the levelling of badland areas, and it is often limited by the most steep *calanchi* sites, where terrain reshaping was not possible. By considering the Corine Land Cover classification (EEA 2007), almost all the *calanchi* badland areas would coincide to shrubby vegetation or bare areas. Therefore, in this case this land-use class represents a water erosion effect and not a cause. As already underlined by Vergari et al. (2011), the factors that may vary in response to environmental changes or economical needs, such as land cover, should be used only if significant changes have not been observed during the time interval considered for the instability landform inventory.

The important anthropic changes that affected the Upper Orcia Valley, aimed at land reclamation, resulted in many badland areas levelling, but they were erased before 1994, the age of the input data. However, these areas maintain some of the environmental factor characteristics that favour intense water erosion processes, as they have been predicted as areas with high and very high water erosion hazard. As a matter of fact, the field survey showed that high erosion rates still persist due to gully and shallow landslide development on cropland. Thus, the performed hazard analysis outlines that badlands could rapidly develop together with their associated very high soil erosion rates, particularly when cropland is abandoned.

This is in accordance with previous studies which confirmed that cropland abandonment in this area, if not followed by efficient land management strategies, can lead to land degradation and soil loss due to a rapid enhancement of piping, gully and shallow landslide development, up to the return to the initial badland conditions (De Alba et al. 2006; Vergari et al. 2013a, b).

## 6 Conclusion

The water erosion hazard assessment in the Upper Orcia Valley was carried out by combining the badland susceptibility analysis to the water erosion rate estimation, performed by means of an empirical statistical method (*Tu* grid analysis) aimed at the evaluation of erosion intensity. The *Tu* grid analysis allowed obtaining the erosion rate estimation map from which the average water erosion rate for *calanchi* areas was deduced. This value was integrated in the spatial prediction of the possible distribution of areas prone to *calanchi* badland development, performed by applying a susceptibility assessment method based on conditional statistical analysis, with the final aim of assessing the water erosion hazard. The analysis

showed that more than 30 % of the study area is prone to very severe denudation processes, being included in the high and very high hazard classes, even if recently development of badlands has frequently been restrained by the agricultural practices. This result outlines how important is the application of appropriate management practices because, when cropland is turned into abandoned, the badlands could rapidly develop.

The susceptibility evaluation was preceded by a bivariate and simple to apply selection of the most important factors controlling the intensity of water erosion processes. A validation procedure was finally applied, in which a random subdivision of *calanchi* badlands was performed. The results confirmed the efficiency of the factor selection procedure, which allowed using few causal factors in the susceptibility analysis without losing information on the indirect influence of the discarded ones.

Moreover, the comparison of the estimated erosion rates with the results of decadal investigations on denudation processes from the study area, deployed by different monitoring methods, confirmed the validity of the proposed erosion hazard assessment method. It represents a useful tool to be applied for soil protection strategy planning in land management, even when direct erosion rate measures are not available.

**Acknowledgments** The author is grateful to Prof. Ion Ionita, one of the Guest Editors, to Dr. Dino Torri and to the other two anonymous reviewers for their precious comments and suggestions that greatly improved the manuscript. The research was funded by the Ministry of Instruction, University and Research (MIUR), PRIN Project 2010–2011 «Dinamica dei sistemi morfoclimatici in risposta ai cambiamenti globali e rischi geomorfologici indotti» (National coordinator C. Baroni, Research Unit coordinator M. Del Monte).

## References

- Acocella V, Rossetti F (2002) The role of extensional tectonics at different crustal levels on granite ascent and emplacement: an example from Tuscany (Italy). *Tectonophysics* 354:71–83
- Akgün A, Türk N (2011) Mapping erosion susceptibility by a multivariate statistical method: a case study from the Ayvalık region, NW Turkey. *Comput Geosci* 37:1515–1524
- Alexander DE (1980) I calanchi, accelerated erosion in Italy. *Geography* 65(2):95–100
- Aucelli PPC, Baldassarre MA, Conforti M, Della Seta M, Roszkopf CM, Scarciglia F, Vergari F (2010) Assessment of present morphodynamics and related erosion rates by means of direct erosion monitoring and digital photogrammetric analysis: the case study of the Upper Orcia Valley (Tuscany, Italy). In: Proceedings of the 1st Italian-Russian workshop on water erosion “slope processes and matter movement” Moscow 2010, Faculty of Geography of the MSU
- Aucelli PPC, Conforti M, Della Seta M, Del Monte M, D’Uva L, Roszkopf CM, Vergari F (2012) Quantitative assessment of soil erosion rates: results from direct monitoring and digital photogrammetric analysis on the Landola catchment in the Upper Orcia Valley (Tuscany, Italy). *Rend Online Soc Geol Ital* 21:1199–1201
- Aucelli PPC, Conforti M, Della Seta M, Del Monte M, D’uva L, Roszkopf CM, Vergari F (2014) Multi-temporal digital photogrammetric analysis for quantitative assessment of soil erosion rates in the Landola catchment of the Upper Orcia Valley (Tuscany, Land Dev Degrad, Italy). doi:10.1002/ldr.2324
- Bagnold RA (1966) An approach to the sediment transport problem from general physics. Geological Survey professional paper 422 I. US Geological Survey, U. S. Government Printing Office
- Baldi P, Bellani S, Ceccarelli A, Fiordalisi A, Squarci P, Taffi L (1994) Correlazioni tra le anomalie termiche ed altri elementi geofisici e strutturali della Toscana meridionale. *Stud Geol Camerti* 1:139–149
- Bonham-Carter GF, Agterberg FP, Wright DF (1989) Weights of evidence modelling: a new approach to mapping mineral potential. In: Agterberg FP, Bonham-Carter GF (eds) *Statistical applications in the earth sciences*, Geological Survey of Canada, pp 171–183
- Bou Kheir R, Wilson J, Deng Y (2007) Use of terrain variables for mapping gully erosion susceptibility in Lebanon. *Earth Surf Process Landf* 32:1770–1782

- Brochet S (1993) Erosion des badlands dans le système Durance-Etang de Berre. Introduction Générale—Aperçu. CEMAGREF—Groupement de Grenoble, Division Protection Contre les Erosions
- Bryan R, Yair A (1982) Perspectives on studies of badland geomorphology. In: Bryan R, Yair A (eds) *Badland geomorphology and piping*. Geobooks, Norwich, pp 1–12
- Bufalo M, Nahon D (1992) Erosional processes of Mediterranean badlands: a new erosivity index for predicting sediment yield from gully erosion. *Geoderma* 52:133–147
- Busoni E, Salvador Sanchis P, Calzolari C, Romagnoli A (1995) Mass movement and erosion hazard patterns by multivariate analysis of landscape integrated data: the Upper Orcia River Valley (Siena, Italy) case. *Catena* 25:169–185
- Calzolari C, Ungaro F (1998) Geomorphic features of a badland (biancane) area (Central Italy): characterization, distribution and quantitative spatial analysis. *Catena* 31:237–256
- Calzolari C, Torri D, Del Sette M, Maccherini S, Bryan R (1997) Evoluzione dei suoli e processi di erosione su biancane: il caso delle biancane de La Foce\_Val d'Orcia, Siena. *Boll Soc Ital Sci Suolo Nuova Ser* 8:185–203
- Cantón Y (1999) Efectos hidrológicos y geomorfológicos de la cubierta y propiedades del suelo en paisaje de cárcavas. Unpublished PhD thesis, Universidad de Almería, Spain
- Carmignani L, Decandia FA, Fantozzi PL, Lazzarotto A, Liotta D, Meccheri M (1994) Tertiary extensional tectonics in Tuscany (northern Apennines, Italy). *Tectonophysics* 238:295–315
- Carrara A, Cardinali M, Guzzetti F, Reichenbach P (1995) GIS technology in mapping landslide hazard. In: Carrara A, Guzzetti F (eds) *Geographical information systems in assessing natural hazards*. Kluwer, Dordrecht, pp 135–176
- Cerdan O, Govers G, Le Bissonnais Y, Van Oost K, Poesen J, Saby N, Gobin A, Vacca A, Quinton J, Auerswald K, Klik A, Kwaad FJPM, Raclot D, Ionita I, Rejman J, Rousseva S, Muxart T, Roxo MJ, Dostal T (2010) Rates and spatial variations of soil erosion in Europe: a study based on erosion plot data. *Geomorphology* 122(1–2):167–177
- Chaplot V, Coadou le Brozec E, Silvera N, Valentin C (2005) Spatial and temporal assessment of linear erosion in catchments under sloping lands of northern Laos. *Catena* 63:167–184
- Chung CJF, Fabbri AG (1999) Probabilistic prediction models for landslide hazard mapping. *Photogramm Eng Remote Sens* 65(12):1389–1399
- Chung CJF, Fabbri AG (2003) Validation of spatial prediction models for landslide hazard mapping. *Nat Hazards* 30(3):451–472. doi:[10.1023/B:NHAZ.0000007172.62651.2b](https://doi.org/10.1023/B:NHAZ.0000007172.62651.2b)
- Ciccacci S, Fredi P, Lupia Palmieri E, Pugliese F (1981) Contributo della analisi geomorfica quantitativa alla valutazione dell'entità dell'erosione nei bacini fluviali. *Boll Soc Geol Ital* 99:455–516
- Ciccacci S, Fredi P, Lupia Palmieri E, Pugliese F (1986) Indirect evaluation of erosion entity in drainage basins through geomorphic, climatic and hydrological parameters. In: Gardiner V (ed) *International geomorphology*. Part II. Wiley, Chichester, pp 33–48
- Ciccacci S, Del Monte M, Marini R (2003) Denudational processes and recent morphological change in a sample area of the Orcia River Upper Basin (Southern Tuscany). *Geogr Fis Din Quat* 26:97–109
- Ciccacci S, Galiano M, Roma MA, Salvatore MC (2008) Morphological analysis and erosion rate evaluation in badlands of Radicofani area (Southern Tuscany—Italy). *Catena* 74:87–97
- Ciccacci S, Galiano M, Roma MA, Salvatore MC (2009) Morphodynamics and morphological changes of the last 50 years in a badland sample area of Southern Tuscany (Italy). *Z Geomorphol N F* 53(3):273–297
- Clerici A, Perego S, Tellini C, Vescovi P (2006) A GIS-based automated procedure for landslide susceptibility mapping by the conditional analysis method: the Baganza valley case study (Italian Northern Apennines). *Environ Geol* 50:941–961
- Clerici A, Perego S, Tellini C, Vescovi P (2010) Landslide failure and runoff susceptibility in the upper T. Ceno valley (Northern Apennines, Italy). *Nat Hazards* 52(1):1–29. doi:[10.1007/s11069-009-9349-4](https://doi.org/10.1007/s11069-009-9349-4)
- Colica A, Guasparri G (1990) Sistemi di fatturazione nelle argille plioceniche del territorio senese. Implicazioni geomorfologiche. *Atti dell'Accademia dei Fisiocritici in Siena* 9:29–36
- Conforti M, Aucelli PPC, Robustelli G, Scarciglia F (2011) Geomorphology and GIS analysis for mapping gully erosion susceptibility in the Turbolo stream catchment (Northern Calabria, Italy). *Nat Hazards* 56:881–898
- Conoscenti C, Di Maggio C, Rotigliano E (2008a) Soil erosion susceptibility assessment and validation using a geostatistical multivariate approach: a test in Southern Sicily. *Nat Hazards* 46:287–305
- Conoscenti C, Di Maggio C, Rotigliano E (2008b) GIS analysis to assess landslide susceptibility in a fluvial basin of NW Sicily (Italy). *Geomorphology* 94(3–4):325–339. doi:[10.1016/j.geomorph.2006.10.039](https://doi.org/10.1016/j.geomorph.2006.10.039)
- Conoscenti C, Agnesi V, Angileri S, Cappadonia C, Rotigliano E, Märker M (2013) A GIS-based approach for gully erosion susceptibility modelling: a test in Sicily. *Environ Earth Sci*, Italy. doi:[10.1007/s12665-012-2205-y](https://doi.org/10.1007/s12665-012-2205-y)

- Conoscenti C, Angileri S, Cappadonia C, Rotigliano E, Agnesi V, Märker M (2014) Gully erosion susceptibility assessment by means of GIS-based logistic regression: a case of Sicily (Italy). *Geomorphology* 204(2014):399–411. doi:10.1016/j.geomorph.2013.08.021
- Cooke RU, Doornkamp JC (1974) *Geomorphology in environmental management*. Clarendon Press, Oxford, p 413
- De Alba S, Borselli L, Torri D, Pellegrini S, Bazzoffi P (2006) Assessment of tillage erosion by mouldboard plough in Tuscany (Italy). *Soil Tillage Res* 85:123–142
- de Vente J, Poesen J, Bazzoffi P, Van Rompaey A, Verstraeten G (2006) Predicting catchment sediment yield in Mediterranean environments: the importance of sediment sources and connectivity in Italian drainage basins. *Earth Surf Process Landf* 31(8):1017–1034
- Del Monte M (2003) Caratteristiche morfometriche e morfodinamiche dell’alto bacino del Fiume Orcia (Toscana meridionale). *Atti XXVIII Cong Geogr Ital*, Roma, pp 1933–1975
- Del Monte M, Fredi P, Lupia Palmieri E, Marini R (2002) Contribution of quantitative geomorphic analysis to the evaluation of geomorphological hazards. In: Allison R (ed) *Applied Geomorphology: theory and practice*. Wiley, Chichester, pp 335–358
- Della Seta M, Del Monte M, Fredi P, Lupia Palmieri E (2004) Quantitative morphotectonic analysis as a tool for detecting deformation patterns in soft rock terrains: a case study from the southern Marches, Italy. *Géomorphologie* 4:267–284
- Della Seta M, Del Monte M, Pascoli A (2005) Quantitative geomorphic analysis to evaluate flood hazards. *Geogr Fis Din Quat* 28(1):117–124
- Della Seta M, Del Monte M, Fredi P, Lupia Palmieri E (2007) Direct and indirect evaluation of denudation rates in Central Italy. *Catena* 71:21–30
- Della Seta M, Del Monte M, Fredi P, Lupia Palmieri E (2009) Space–time variability of denudation rates at the catchment and hillslope scales on the Tyrrhenian side of Central Italy. *Geomorphology* 107:161–177
- Desmet PJJ, Poesen J, Govers G, Vandaele K (1999) Importance of slope gradient and contributing area for optimal prediction of the initiation and trajectory of ephemeral gullies. *Catena* 37:377–392
- EEA (2007) CLC2006 technical guidelines. EEA Technical report no. 17/2007
- Fairbridge RW (1968) *Encyclopedia of geomorphology*. Reinhold Book, New York
- Farabollini P, Gentili B, Pambianchi G (1992) Contributo allo studio dei calanchi: due aree campione nelle Marche. *Stud Geol Camerti* 12:105–115
- Florinsky IV (2012) *Digital terrain analysis in soil science and geology*. Elsevier/Academic Press, Amsterdam. ISBN:978-0-12-385036-2
- Gallart F, Solé A, Puigdefàbregas J, Lázaro R (2002) Badland systems in the Mediterranean. In: Bull LJ, Kirkby MJ (eds) *Dryland rivers: hydrology and geomorphology of semi-arid channels*. Wiley, London, pp 299–326
- García-Ruiz JM, López-Bermudez F (2009) Un caso especial: badlands y sufosión. In: Sociedad Española de Geomorfología (ed) *Erosión del suelo en España*, Zaragoza SEG 239–72
- García-Ruiz JM, Beguería S, Nadal-Romero E, González-Hidalgo JC, Lana-Renault N, Sanjuán Y (2015) A meta-analysis of soil erosion rates across the world. *Geomorphology* 239:160–173
- Gini C (1914) Sulla misura della concentrazione e della variabilità dei caratteri. *Atti del Regio Istituto Veneto di Scienze, Lettere e Arti*, LXXIII(parte II), pp 1203–1248
- Gómez Gutiérrez Á, Schnabel S, Felicísimo ÁM (2009a) Modelling the occurrence of gullies in rangelands of southwest Spain. *Earth Surf Process Landf* 34:1894–1902
- Gómez Gutiérrez Á, Schnabel SJ, Contador FL (2009b) Using and comparing two nonparametric methods (CART and MARS) to model the potential distribution of gullies. *Ecol Model* 220:3630–3637
- Grimm M, Jones RJA, Montanarella L (2003) *Soil erosion risk in Europe*. European Soil Bureau Institute for Environment & Sustainability JRC Ispra, Ispra
- Irigaray Fernández C, Fernández Del Castillo T, El Hamdouni R, Chacón Montero J (1999) Verification of landslide susceptibility mapping: a case study. *Earth Surf Proc Landf* 24:537–544
- Jenks GF (1967) The data model concept in statistical mapping. *Int Yearbook Cartogr* 7:186–190
- Kakembo V, Xanga WW, Rowntree K (2009) Topographic thresholds in gully development on the hillslopes of communal areas in Ngqushwa Local Municipality, Eastern Cape, South Africa. *Geomorphology* 110:188–194
- Kirkby MJ, Atkinson K, Lockwood J (1990) Aspect, vegetation cover and erosion on semi-arid hillslopes. In: Thornes J (ed) *Vegetation and erosion*. Wiley, Chichester, pp 25–39
- Liotta D (1996) Analisi del settore centromeridionale del bacino pliocenico di Radicofani (Toscana meridionale). *Boll Soc Geol Ital* 115:115–143
- Lorenz MO (1905) Methods of measuring the concentration of wealth. *Publ Am Stat As* 9(70):209–219

- Lucà F, Conforti M, Robustelli G (2011) Comparison of GIS-based gully susceptibility mapping using bivariate and multivariate statistics: Northern Calabria, South Italy. *Geomorphology* 134:297–308
- Lupia Palmieri E (1983) Il problema della valutazione dell'entità dell'erosione nei bacini fluviali. In: *Atti del XXIII Congresso Geografico Italiano II*, pp 143–176
- Lupia Palmieri E, Centamore E, Ciccacci S, D'Alessandro L, Del Monte M, Fredi P, Pugliese F (2001) Geomorfologia quantitativa e morfodinamica del territorio abruzzese. III—Il bacino idrografico del Fiume Saline. *Geogr Fis Dinam Quat* 24(2):157–176
- Maerker M, Della Seta M, Vergari F, Del Monte M (2012) Process-based assessment of erosion dynamics in the Upper Orcia Valley (Southern Tuscany, Italy): a new semiquantitative integrated approach. *Rend Online Soc Geol Ital* 21:1208–1211
- Maetens W, Vanmaercke M, Poesen J, Jankauskas B, Jankauskiene G, Ionita I (2012) Effects of land use on annual runoff and soil loss in Europe and the Mediterranean: a meta-analysis of plot data. *Prog Phys Geogr* 36(5):599–653
- Magliulo P (2010) Soil erosion susceptibility maps of the Janare Torrent Basin (Southern Italy). *J Maps* 6:435–447
- Magliulo P (2012) Assessing the susceptibility to water-induced soil erosion using a geomorphological, bivariate statistics-based approach. *Environ Earth Sci* 67:1801–1820
- Märker M, Flügel WA, Rodolfi G (1999) Das Konzept der “Erosions Response Units” (ERU) und seine Anwendung am Beispiel des semi-ariden Mkomazi-Einzugsgebietes in der Provinz Kwazulu/Natal, Südafrika. In: *Tübinger Geowissenschaftliche Studien, Reihe D.: Geoökologie und Quartaerforschung. Angewandte Studien zu Massenverlagerungen*, Tübingen
- Märker M, Pelacani S, Schröder B (2011) A functional entity approach to predict soil erosion processes in a small Plio-Pleistocene Mediterranean catchment in Northern Chianti, Italy. *Geomorphology* 125:530–540
- Martínez-Carreras N, Soler M, Hernández E, Gallart F (2007) Simulating badland erosion with KINEROS2 in a small Mediterranean mountain basin (Vallcebre, Eastern Pyrenees). *Catena* 71:145–154
- Martínez-Casasnovas JA, Poch RM (1998) Estado de conservación de los suelos de la cuenca del embalse Joaquín Costa. *Limnetica* 14:83–91
- Meyer A, Martínez-Casasnovas JA (1999) Prediction of existing gully erosion in vineyard parcels of the NE Spain: a logistic modelling approach. *Soil Tillage Res* 50:319–331
- Montgomery DR, Dietrich WE (1992) Channel initiation and the problem of landscape scale. *Science* 255:826–830
- Moore ID, Grayson RB, Ladson AR (1991) Digital terrain modeling: a review of hydrological, geomorphological, and biological applications. *Hydrol Process* 5:3–30
- Moretti S, Rodolfi G (2000) A typical “calanchi” landscape on the Eastern Apennine margin (Atri, Central Italy): geomorphological features and evolution. *Catena* 40:217–228
- Morgan RPC (2005) *Soil erosion and conservation*, 3rd edn. Blackwell, Oxford. ISBN:1-4051-1781-8
- Nadal-Romero E, Regúés D (2010) Geomorphological dynamics of subhumid mountain badland areas—weathering, hydrological and suspended sediment transport processes: a case study in the Aragón catchment (Central Pyrenees) and implications for altered hydroclimatic regimes. *Prog Phys Geogr* 34(2):123–150
- Nadal-Romero E, Latron J, Martí-Bono C, Regúés D (2008) Temporal distribution of suspended sediment transport in a humid Mediterranean badland area: the Aragón catchment, Central Pyrenees. *Geomorphology* 97:601–616
- Nadal-Romero E, Martínez-Murillo JF, Vanmaercke M, Poesen J (2011) Scale dependency of sediment yield from badland areas in Mediterranean environments. *Prog Phys Geogr* 35(3):297–332
- Nadal-Romero E, Petric K, Verachtert E, Bochet E, Poesen J (2014) Effects of slope angle and aspect on plant cover and species richness in a humid Mediterranean badland. *Earth Surf Proc Land* 39(13):1705–1716
- Nazari Samani A, Ahmadi H, Jafari M, Boggs G, Ghoddousi J, Malekian A (2009) Geomorphic threshold conditions for gully erosion in Southwestern Iran (Boushehr–Samal watershed). *J Asian Earth Sci* 35:180–189
- Nefeslioglu HA, Duman TY, Durmaz S (2008) Landslide susceptibility mapping for a part of tectonic Kelkit Valley (Eastern Black Sea region of Turkey). *Geomorphology* 94:401–418. doi:10.1016/j.geomorph.2006.10.036
- Nogueras P, Burjachs F, Gallart F, Puigdefabregas J (2000) Recent gully erosion in the El Cautivo badlands (Tabernas, SE Spain). *Catena* 40:203–215
- Piccarreta M, Capolongo D, Miccoli MN, Bentivenga M (2012) Global change and long-term gully sediment production dynamics in Basilicata, southern Italy 01/2012. *Environ Earth Sci* 67:1619–1630



- Regués D, Balasch JC, Castellort X, Soler M, Gallart F (2000a) Relación entre las tendencias temporales de producción y transporte de sedimentos y las condiciones climáticas en una pequeña cuenca de montaña mediterránea (Vallcebre, Pirineos orientales). *Cuad Investig Geogr* 2:41–65
- Regués D, Guàrdia R, Gallart F (2000b) Geomorphic agents versus vegetation spreading as causes of badland occurrence in a Mediterranean subhumid mountainous area. *Catena* 40:173–187
- Remondo J, Gonzáles A, Díaz de Terán JR, Cendrero A, Fabbri A, Chung CJF (2003) Validation of landslide susceptibility maps. Examples and applications from a case study in Northern Spain. *Nat Hazards* 30(3):437–449. doi:10.1023/B:NHAZ.0000007201.80743.fc
- Richard D, Mathys S (1999) Historique, contexte technique et scientifique des BVRE de Draix. Caractéristiques, données disponibles et principaux résultats acquis au cours de dix ans de suivi. In: Mathys N (ed) Les bassins versants expérimentaux de Draix, Laboratoire d'étude de l'érosion en montagne, Cemagref Antony, pp 11–28
- Rodolfi G, Frascati F (1979) Cartografia di base per la programmazione degli interventi in aree marginali (Area rappresentativa Alta Val D'Era). *Annali Ist. sper. Studio e Difesa Suolo*, vol 10
- Sirvent J, Desir G, Gutiérrez M, Sancho C, Benito G (1997) Erosion rates in badlands areas recorded by collectors, erosion pins and profilometer techniques (Ebro Basin, NE-Spain). *Geomorphology* 18:61–75
- Solé A, Calvo A, Cerdà A, Lázaro R, Pini R, Barbero J (1997) Influence of micro-relief patterns and plant cover on runoff related processes in badlands from Tabernas (SE Spain). *Catena* 31:23–38
- Svoray T, Mikhailov E, Cohen A, Rokah L, Sturm A (2012) Predicting gully initiation: comparing data mining techniques, analytical hierarchy processes and the topographic threshold. *Earth Surf Process Landf* 37:607–619
- Torri D, Bryan RB (1997) Micropiping processes and biancane evolution in Southeast Tuscany, Italy. *Geomorphology* 20:219–235
- Torri D, Poesen J (2014) A review of topographic threshold conditions for gully head development in different environments. *Earth Sci Rev* 130:73–85
- Torri D, Colica A, Rockwell D (1994) Preliminary study of the erosion mechanisms in a biancana badland (Tuscany, Italy). *Catena* 23:281–294
- Torri D, Calzolari C, Rodolfi G (2000) Badlands in changing environments: an introduction. *Catena* 40:119–125
- Torri D, Borselli L, Calzolari C, Yañez MS, Salvador Sanchis MP (2002) Soil erosion, land use, soil qualities and soil functions: effects of erosion. In Rubio JL, Morgan RPC, Asins S, Andreu V (eds) Proceedings of the third International Congress Man and Soil at the Third Millennium, 2002, Geofoma Ediciones
- Torri D, Santi E, Marignani M, Rossi M, Borselli L, Maccherini S (2013) The recurring cycles of biancana badlands: erosion, vegetation and human impact. *Catena* 106:22–30
- Van Rompaey A, Bazzoffi P, Jones RJA, Montanarella L (2005) Modeling sediment yields in Italian catchments. *Geomorphology* 65(1–2):157–169
- Vergari F, Della Seta M, Del Monte M, Fredi P, Lupia Palmieri E (2011) Landslide susceptibility assessment in the Upper Orcia Valley (Southern Tuscany, Italy) through conditional analysis: a contribution to the unbiased selection of causal factors. *Nat Hazards Earth Syst Sci* 11:1475–1497
- Vergari F, Della Seta M, Del Monte M, Barbieri M (2013a) Badlands denudation “hot spots”: the role of parent material properties on geomorphic processes in 20-years monitored sites of Southern Tuscany (Italy). *Catena* 106:31–41
- Vergari F, Della Seta M, Del Monte M, Fredi P, Lupia Palmieri E (2013b) Long- and short-term evolution of several Mediterranean denudation hot spots: the role of rainfall variations and human impact. *Geomorphology* 183:14–27
- Vergari F, Della Seta M, Del Monte M, Pieri L, Ventura F (2014) Integrated approach to the evaluation of denudation rates in an experimental catchment of the Northern Italian Apennines. In: Lollino G, Manconi A, Clague J, Shan W, Chiarle M (eds) Engineering geology for society and territory. Volume 1: Climate change and engineering geology. Springer, Berlin, pp 533–537
- Wilson JP, Gallant JC (2000) Terrain analysis: principles and applications. Wiley, Canada
- Yair A, Lavee H (1985) Runoff generation in arid and semiarid zones. In: Anderson MG, Burt TP (eds) Hydrological forecasting. Wiley, Chichester, pp 183–220
- Yang CT, Stall JB (1974) Unit stream power for sediment transport in natural rivers. WRC research report no. 88
- Zachar D (1982) Soil erosion. Elsevier, Amsterdam
- Zêzere JL, Trigo RM, Trigo IF (2004) Shallow and deep landslides induced by rainfall in the Lisbon region (Portugal): assessment of relationships with the North Atlantic Oscillation Source. *Nat Hazards Earth Syst* 5(3):331–344